SAR and QSAR in Environmental Research

Publication details, including instructions for authors and subscription information:
http://www.tandfonline.com/loi/gsar20

Homology modelling of the Apis mellifera nicotinic acetylcholine receptor (nAChR) and docking of imidacloprid and fipronil insecticides and their metabolites

A. Rocher [a] & N. Marchand-Geneste [a]

[a] CNRS UMR 5255 ISM-LPTC, Université Bordeaux 1, Talence Cedex, France

Published online: 04 Dec 2010.

To cite this article: A. Rocher & N. Marchand-Geneste (2008): Homology modelling of the Apis mellifera nicotinic acetylcholine receptor (nAChR) and docking of imidacloprid and fipronil insecticides and their metabolites, SAR and QSAR in Environmental Research, 19:3-4, 245-261

To link to this article: http://dx.doi.org/10.1080/10629360802083731

SAR and QSAR in Environmental Research
Vol. 19, Nos. 3–4, April–June 2008, 245–261

Taylor & Francis
Taylor & Francis Group

Homology modelling of the *Apis mellifera* nicotinic acetylcholine receptor (nAChR) and docking of imidacloprid and fipronil insecticides and their metabolites

A. Rocher and N. Marchand-Geneste*

CNRS UMR 5255 ISM-LPTC, Université Bordeaux 1, Talence Cedex, France

(*Received 4 July 2007; In final form 18 February 2008*)

Five homology models for honeybee (*Apis mellifera*) nicotinic acetylcholine receptor (nAChR) $\alpha1/\beta1$, $\alpha3/\beta2$, $\alpha4/\beta2$, $\alpha6/\beta2$ and $\alpha9/\alpha9$ subtypes were built from the *Torpedo marmorata* nAChR X-ray structure. Then, imidacloprid, fipronil and their metabolites were docked into the ligand binding domain (LBD) of these receptors and the corresponding scoring functions were calculated. The binding modes of the docked compounds were carefully analysed. Finally, multivariate analyses were used for deriving structure-activity relationships based on hydrogen bond number and scoring functions between the insecticides and the nAChR models.

Keywords: nicotinic acetylcholine receptor; *Apis mellifera*; imidacloprid; fipronil; homology modelling; docking; QSAR

1. Introduction

The nicotinic acetylcholine receptors (nAChR), which are present in insect nervous tissues, are the targets of neonicotinoid insecticides [1]. This newest major group of insecticides is used against piercing-sucking pests (aphids, leafhoppers and white-flies). These insecticides act on transmission of the nervous message and lead quickly to the paralysis of the insect. These nAChR agonists are supposed to be more toxic towards insects than mammals, but this toxicity concerns pollinator insects such as *Apis mellifera* [2]. The use of imidacloprid (Gaucho® from Bayer) on sunflowers was forbidden in France in 1999 because of the high hazard to bees. However after this step, the honeybee deaths persisted. In 2004, the French government suspended the use of Gaucho for treatment of maize-seeds; this suspension applies only to France. The controversy surrounding the use of Gaucho is still active, especially since another pesticide, fipronil (Regent® from Aventis), a second-generation phenylpyrazole insecticide, which is a potent inhibitor of the gamma-aminobutyric acid (GABA)-gated chloride channel, was also incriminated and suspended. To date, the use of insecticides containing imidacloprid (neonicotinoid) or fipronil (phenylpyrazole) is still forbidden in France. Studies have shown that imidacloprid (and some of its metabolites) and fipronil are highly toxic toward *A. mellifera* and can alter the bee foraging and learning [3,4].

The purpose of this study was to model the 3D structure of *A. mellifera* nACh receptors for different subunits (no crystal structures are available for nAChR). The design

*Corresponding author. Email: n.geneste@ism.u-bordeaux1.fr

ISSN 1062–936X print/ISSN 1029–046X online

DOI: 10.1080/10629360802083731
http://www.informaworld.com

of such models is necessary to better understand the interactions between the insecticides/metabolites and the nACh receptors. To achieve such goals, homology models of *A. mellifera* nAChR $\alpha1/\beta1$, $\alpha3/\beta2$, $\alpha4/\beta2$, $\alpha6/\beta2$ and $\alpha9/\alpha9$ LBDs were built with a resolved crystallographic structure of *Torpedo marmorata* nAChR as template [5]. This homology modelling was performed with the free Swiss-PdbViewer software connected with the SWISS-MODEL Internet server [6]. Secondly, docking studies were performed for selected insecticides and metabolites using LigandFit module of Cerius^2, and scoring functions were calculated for the best poses (positions and orientations) [7]. The molecular interactions between insecticides/metabolites and nACh receptor LBD of *A. mellifera* were carefully analysed. Finally, some multivariate analyses were performed between LD_{50} values and simple descriptors from the docking analysis such as the number of hydrogen bonds and the scoring functions.

2. Receptor and insecticide structures and functions

2.1 *The ligand-gated ion channel family*

Ligand-gated ion channels (LGICs) are a protein super family that includes the receptors for the excitatory amino-acid glutamate and aspartate, the inhibitory amino-acid GABA and glycine, as well as the serotonin 5-HT_3 receptor. The nAChR is an LGIC responsible for rapid neurotransmission at neuromuscular junctions and at some sites of the central nervous system (CNS) [8]. LGICs comprise an extracellular LBD and an ion-channel domain that is integrated to the membrane. The structure is made up of five protein subunits arranged in a circle to form a pore, or a channel, that remains closed until its specific ligand binds to the recognition site. Distinct nAChR subtypes (neuronal or muscular) exist assembled as five subunits (α, β, γ, δ and ε), which can lead to homopentamer or heteropentamer receptors [4,9]. They can all be stimulated by the acetylcholine neurotransmitter or the nicotine alkaloid. The neuronal type receptors are constituted of α and β subunits within binding sites at the interface between two subunits. To date, seven *A. mellifera* nAChR α subunits ($\alpha1$, $\alpha2$, $\alpha3$, $\alpha4$, $\alpha6$, $\alpha7$ and $\alpha9$) and two β subunits ($\beta1$ and $\beta2$) have been sequenced [10–12]. They play roles in learning and memory, olfactory signal processing, mechanosensory antennal input, and visual processing. No crystallographic structure has been resolved for the *A. mellifera* nAChR. However, some studies built the 3D structure of human nAChR using sequence homology with the *Lymnae stagnalis* nAChPB X-ray structure [13–15].

2.2 *Imidacloprid and fipronil insecticides*

Many neonicotinoid insecticides act at the binding site of insect nAChRs. One of them, imidacloprid, is used as the active component for the treatment of seeds (Gaucho®). Imidacloprid interferes with the transmission of stimuli in the CNS of the insect. Specifically, it causes a blockade in a type of neuronal pathway (nicotinergic) that is more abundant in insects than in warm-blooded animals. This blockage leads to the accumulation of the neurotransmitter acetylcholine, resulting in the paralysis, and eventually in the death of the insects. Fipronil is also a disruptor of the insect CNS via the $GABA_A$ receptor, acting by contact and action on the stomach. It blocks the GABA-gated chloride channels of neurons in the CNS, resulting in neuronal excitation and death of the insect.

Table 1. Observed LD_{50} values of neonicotinoids and metabolites for *A. mellifera* [17,18].

Compounds	*Imidacloprid (Imi)*	*5OHImi*	*DiOHImi*	*Olefin*	*Urea*	*6CNA**	*Fipronil (Fip)*
LD_{50} ng/bee	41	159	>49	>36	>99500	>121500	6

Note: *Acid 6-cyanochloronicotinic.

3. Materials and methods

3.1 *Toxicity*

The insecticide metabolites have not been studied a lot [3,16]. The imidacloprid metabolites conserve a chloropyridinyl part like the olefin-imidacloprid, the epoxy-imidacloprid, the urea, the 6-cyanochloronicotinic acid, the 4-hydroxy, the 5-hydroxy and the dihydroxy-imidacloprid (Table 1, Figure 1). Those of fipronil maintain both their aromatic and amino-pyrazole cycle: MB45897, MB45950, MB46136, MB46400, desulfinyl-fipronil, RPA104615, RPA105048, RPA105320, RPA200761, and RPA200766 (Figure 1). Table 1 shows the toxicity of imidacloprid, fipronil and some metabolites for *A. mellifera*. These toxicities are evaluated with the 48h oral LD_{50} [17,18].

3.2 *Molecular modelling*

Molecular structures of insecticides (Figure 1) were built and minimised with the AM1/RHF semi-empirical method using AMPAC 8.16 [19]. To have an accurate estimation of the C–S bond length, fipronil and metabolite geometries were optimised with B3LYP/6-31G(d) level of calculation using Gaussian 98 [20]. To validate the choice of the semi-empirical method used to optimise the insecticide geometries (i.e., the AM1 hamiltonian), a confrontation with existing X-ray structures of insecticides (e.g., imidacloprid, MB45950 and desulfinyl fipronil) has been undertaken. Hence, the superposition of the imidacloprid optimised structure with the crystallographic structure extracted from the Cambridge Crystallographic Structure Database was performed and leads to a root mean square (RMS) deviation of about 0.44 Å [21]. Moreover, all bond lengths have comparable values, and the only difference found was the dihedral angle between the two cycles.

3.3 *Homology modelling*

Homology modelling was performed using Swiss-PdbViewer freeware, which is linked to the Internet SWISS-MODEL Web server [6,22].

3.3.1 *Sequence alignment*

The *A. mellifera* nAChR sequences (Table 2, Figure 2(a)) were obtained from the ExPASy Molecular Biology Server using TrEMBL/Swiss-Prot databank [11,12,23,24]. The sequence alignment and the homology modelling were based on the crystal structure of the *T. marmorata* nAChR (PDB entry: 2BG9, 4 Å resolution) using the chains A and B [5,6]. The 2BG9 structure was selected because it is currently the most recent and accurate resolved X-ray structure. The LBD sequences of the *A. mellifera* nAChR subunits and the

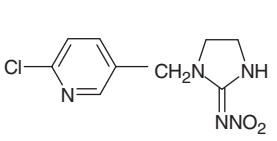

Imidacloprid (Imi)

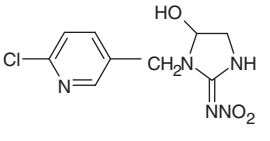

5-hydroxy-imidacloprid (5OHImi)

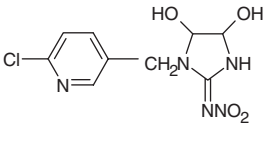

Dihydroxy-imidacloprid (DiOHImi)

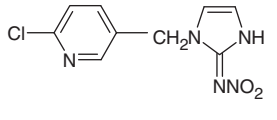

Olefin-imidacloprid (Olefin)

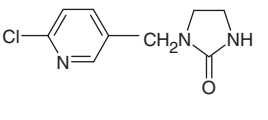

Urea-imidacloprid (Urea)

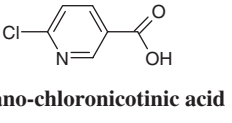

6-cyano-chloronicotinic acid (6CNA)

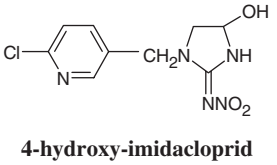

4-hydroxy-imidacloprid (4OHImi)

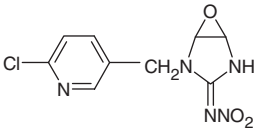

Epoxy-imidacloprid (Epoxy)

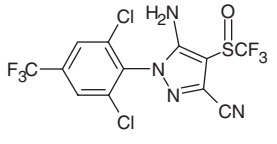

Fipronil (Fip)

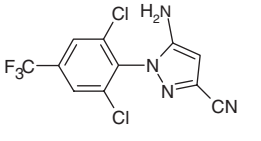

MB45897 (Met 1)

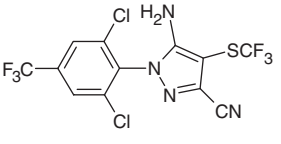

MB45950 (Met 2)

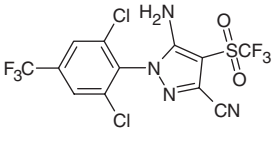

MB46136 (Met 3)

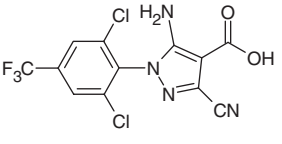

MB46400 (Met 4)

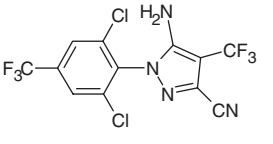

Desulfinyl-fipronil (Met 5)

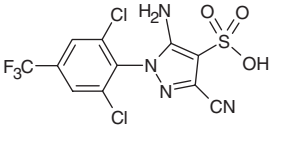

RPA104615 (Met 6)

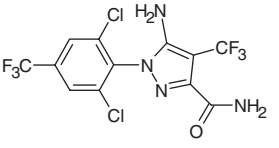

RPA105048 (Met 7)

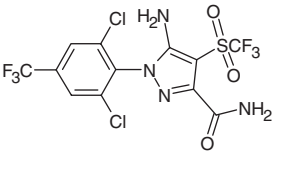

RPA105320 (Met 8)

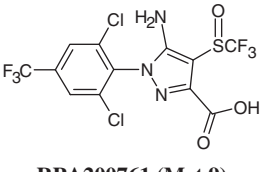

RPA200761 (Met 9)

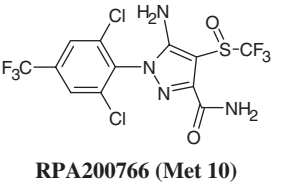

RPA200766 (Met 10)

Figure 1. Structures of compounds used in the docking studies.

Table 2. Primary sequences of *A. mellifera* nAChR α and β subtypes.

FASTA format	*Subunit equivalent*	*Type of subunit*
A0EIZ1	nAChR α1	Muscle
A0EIZ2	nAChR α3	Neuronal
A0EIZ3	nAChR α4	Neuronal
A0EIZ5	nAChR α6	Neuronal
A0EIZ7	nAChR α9	Neuronal
A0EIZ8	nAChR β1	Muscle
A0EIZ9	nAChR β2	Neuronal

T. marmorata nAChR A/B (A is α-type chain and B a β-type) were aligned using CLUSTALW, and a manual refinement was performed to reduce the largest gaps [25].

The following *A. mellifera* nAChR subunits were built: $\alpha3/\beta2$, $\alpha4/\beta2$, $\alpha6/\beta2$, $\alpha1/\beta1$ and $\alpha9/\alpha9$.

3.3.2 *Homology model construction*

The sequence alignment allowed us to assign the *T. marmorata* residue coordinates to the honeybee residues for the regions of greatest structural conservation. The Internet server SWISS-MODEL and the Swiss-PdbViewer software screened the models for unfavourable steric contacts and the side chains were corrected when necessary using the Swiss-PdbViewer rotamer library database.

3.3.3 *Model refinement*

The homology model obtained for each subunit (e.g., Apis_nAChR$\alpha3\beta2$) was energy minimised by SWISS-MODEL using the GROMOS96 force field [26]. To have consistency between all the molecular modelling modules used for this study, all the comparative models built with SWISS-MODEL server were then energy minimised with the steepest descent method of the DISCOVER module of InsightII using the Consistent Valence Force Field (CVFF) [27]. These models were further subjected to energy minimisation with the conjugate gradient technique leading to refined 3D structures.

3.4 *Docking studies*

The docking program used in this study was the shape-based method LigandFit available from the Accelrys Cerius^2 package, which considers the receptor as fixed and the ligand as flexible [28]. A flood-filling algorithm was used to locate the binding site or site model, and a conformational search technique based on a Monte Carlo method generated every possible ligand conformers. Then, the affinity between the ligand and the protein was evaluated with scoring functions, which calculated free binding interaction energies based on molecular force field terms. Among all the existing scoring functions, none can estimate all types of interaction between ligand and protein. Five scoring functions were then computed: Ligscore 1 and 2, JAIN and PMF [29–32]. All calculations were performed on a Silicon Graphics Octane (SGI) workstation using InsightII and Cerius^2 molecular modelling software packages available from Accelrys Inc. [7,33].

(a) **A0EIZ2: A0EIZ2_APIME**

```
>A0EIZ2|A0EIZ2_APIME Nicotinic acetylcholine receptor alpha3 -  Apis mellifera
(Honeybee).
    1         11        21        31        41        51
1   MMKSLVGIMWIVLVLISGCSGNPDAKRLYDDLLSNYNKLVRPVVNVTDALTVKIKLKLSQ 60
61  LIDVNLKNQIMTTNLWVEQSWYDYKLKWDPKEYGGVEMLHVPSDHIWRPDIVLYNNADGN 120
121 FEVTLATKATLNYTGRVEWKPPAIYKSSCEIDVEYFPFDEQTCVMKFGSWTYDGFQVDLR 180
181 HIDEIRGKNVVDIGVDLSEFYTSVEWDILEVPAVRNEKFYTCCDEPYLDITFNITMRRKT 240
241 LFYTVNLIIPCMGISFLTVLVFYLPSDSGEKVSLSISILLSLTVFFLLLAEIIPPTSLVV 300
301 PLLGKFVLFTMILDTFSICVTVVVLNVHFRSPQTHVMAPWVRRVFIHVLPRLLVMRRYNT 360
361 PSKRSDYDSRPQYQIDKRSMGSHHGQRVMVRTCNGLELRDPSLFVETSASELVESSVLFP 420
421 SLDSRDELHPRELEAVNLGSACRIHGSPATTAAPPQLPTEESVDALCNTLHHWHHCPEIY 480
481 KAIEGIRFIADHTKREEDSTRVKEDWKYVAMVLDRLFLWIFTLAVVVGTAGIILQAPTLY 540
541 DDRIPIDVRLSEIASTTAKPHIVTSL
```

A0EIZ9: A0EIZ9_APIME

```
>A0EIZ9|A0EIZ9_APIME Nicotinic acetylcholine receptor beta2 -  Apis mellifera
(Honeybee).
    1          11          21          31          41          51
1   MLNMKNIFPV  LFVIINVLLH  GQVICFVCKD  ITSTSALYRL  KLYLFCDYDR  DIIPEQKNAT  60
61  KIDFGLSIQH  YNVDEYSHTV  DFHVMLKLMW  EQSHLTWKSS  EFDSINSIRV  KSYEIWVPDI  120
121 VMHSVTSVGI  DLEMPSVECI  VFNSGTILCV  PFTTYTPVCE  YDHTWWPYDI  LNCTIHIASW  180
181 SHGSNEIKLN  SLDTEQILDD  MYNNNTEWEI  VHMSHSESTI  DSKFGLGFTT  DLLSYNILLR  240
241 RHYSMNSTTY  VTLTIVLMTM  TLMTLWLEPS  STERMIIANL  NFILHLFCLL  DVQWRIPFNG  300
301 IQMPNLMVFY  EKSLALAAFS  LMLTSILRYL  QELHVDAPTW  ISSVTESVLK  SKIGQVFLIT  360
361 ILDSKVSARI  EMNEDDNTSL  VSLDKKQYTW  RHTSVLIGWS  AFLCISLVYI  IMLIIFIPRN  420
421 IYENFIS
```

(b) **Manual Alignment Swiss-PdbViewer**

```
A3B2_APIS   1   NPDAKRLYDD LLSNYNKLVR PVVNVTDALT VKIKLKLSQL IDVNLKNQIM
2BG9AB      1   SEHETRLVAN LLENYNKVIR PVEHHTHFVD ITVGLQLIQL INVDEVNQIV
                .    **  . ** ****..* ** . *  .  . . * * ** *.*.  ***.

A3B2_APIS  51   TTNLWVEQSW YDYKLKWDPK EYGGVEMLHV PSDHIWRPDI VLYNNADGNF
2BG9AB     51   ETNVRLRQQW IDVRLRWNPA DYGGIKKIRL PSDDVWLPDL VLYNNADGDF
                 **... * *  * .*.*.*  .***. .... *** .* **. ********.*

A3B2_APIS 101   EVTLATKATL NYTGRVEWKP PAIYKSSCEI DVEYFPFDEQ TCVMKFGSWT
2BG9AB    101   AIVHMTKLLL DYTGKIMWTP PAIFKSYCEI IVTHFPFDQQ NCTMKLGIWT
                 .   **  * .***.. * * ***.** ***  *  ****.*  * **.* **

A3B2_APIS 151   YDGFQVDLRH IDEIRGKNVV DI-GVDLSEF YTSVEWDILE VPAVRNEKFY
2BG9AB    151   YDGTKVSISP ESD-RPD-LS TFMESGEWVM KDYRGWKHWV YYTCCPDTPY
                ***  * .     . *   .   .               *       .   .  *

A3B2_APIS 200   TCCDEPYLDI TFTSALYRLK LYLFCDYDRD IIPEQK-NAT -KIDFGLSIQ
2BG9AB    199   LDITYHFIMQ RISVMEDTLL SVLFENYNPK VRPSQTVGDK VTVRVGLTLT
                      ..    ..     *    ** .*.   . * *         .  **..

A3B2_APIS 248   HYNV-DEYSH TVDFHVMLKL MWEQSHLTWK SSEFDSINSI RVKSYEIWVP
2BG9AB     39   SLLILNEKNE EMTTSVFLNL AWTDYRLQWD PAAYEGIKDL SIPSDDVWQP
                   . .* .   .   * *.*  * . .* *  .. ...*. .  . * ..* *

A3B2_APIS 297   DIVMHSVTSV GIDLEMPSVE CIVFNSGTIL CVPFTTYTPV CEYDHTWWPY
2BG9AB     89   DIVLMNNNDG SFEITLH-VN VLVQHTGAVS WHPSAIYRSS CTIKVMYFPF
                ***. .     .... .  *.  .* ..*..    * . * .  *       *.

A3B2_APIS 347   DILNCTIHIA SWSHGSNEIK LNSLDTEQIL DDMYNNNTEW EIVHMSHSES
2BG9AB    138   DWQNCTMVFK SYTYDTSEVI LQHALDAMIN QDAFTENGQW SIEHK-PSRK
                *  ***. .  * .  ..*.  *       *  .* . .* .*  * *.  *

A3B2_APIS 397   TIDSKFGLGF TTDLLSYNIL LRR
2BG9AB    196   N-WRSDDPSY -EDVTFYLII QRK
                    ..   *.  * *.  *.
```

Figure 2. (a) *A. mellifera* nAChR α3 and β2 sequences obtained from TrEMBL/Swiss-Prot. The LBD is represented in bold; (b) Sequence alignment of *A. mellifera* nAChR α3/β2 and *T. marmorata* (2BG9) nAChR A/B ligand binding domain. Stars are under identical amino acids and dots under similar.

Table 3. Sequence identities and similarities between α and β subunits of *A. mellifera* nAChR and *T. marmorata* nAChR obtained by manual alignment.

Target sequence	*% of identity*	*% of similarity*	*Reference sequence*
A0EIZ1 (α1)	42.4	65.7	2BG9A
A0EIZ2 (α3)	38.9	58.8	2BG9A
A0EIZ3 (α4)	44.5	73.0	2BG9A
A0EIZ5 (α6)	41.2	79.1	2BG9A
A0EIZ7 (α9)	25.9	65.1	2BG9A
A0EIZ8 (β1)	44.8	61.4	2BG9B
A0EIZ9 (β2)	22.6	49.5	2BG9B

4. Results and discussion

4.1 *Homology models*

The five homology models of *A. mellifera* nAChR were built with the following subunits: $\alpha3/\beta2$, $\alpha4/\beta2$, $\alpha6/\beta2$, $\alpha1/\beta1$ and $\alpha9/\alpha9$. In this section, the computational details are reported only for the nAChR $\alpha3/\beta2$. Figure 2(b) illustrates the LBD sequence alignment of *A. mellifera* nAChR $\alpha3/\beta2$ and *T. marmorata* nAChR A/B permitting us to construct the Apis_nAChR$\alpha3\beta2$ model. This alignment reveals a medium level of sequence conservation between the two receptors with 31% of identity and 54% of similarity. Table 3 shows the sequence identities and similarities obtained from pairwise sequence alignment of 2BG9 with the five nAChR of α and β subunits. It also reveals that $\alpha4$ and $\beta1$ subunits show the best pairwise alignment with more than 44% of identity with 2BG9 chains. The $\alpha9$ subunit presents a low identity (25.9%) but a high similarity (65.1%) with the A chain of 2BG9. The $\beta2$ subunit seems to be the most different subunits with the lowest identity percentage (22.6%).

The superposition of the backbone of Apis_nAChR$\alpha3\beta2$ comparative model with that of *T. marmorata* nAChR A/B shows minimal deviation. It was noted that the RMS deviation between Cα atoms in the aligned position is 0.33 Å suggesting that the LBDs of the two species are similar. The secondary structure of the $\alpha3/\beta2$ model is displayed in Figure 3. A superposition with the X-ray structure of nAChBP complexed with nicotine (PBD entry: 1UW6) allowed us to locate the binding site at the interface of the α and β chains [13]. It was worthy to note that this latter superposition led to significant conformational differences between both structures. Moreover in a previous study, a 3D model of human nAChR $\alpha3\beta2$ was constructed from the *T. marmorata* nAChR A/B template and was compared to the 3D comparative model reported by Dutertre et al., which was built from nAChBP X-ray structure as template [15,34,35]. The superposition of these two human nAChR comparative models underlined important differences inside the active site: a larger cavity was observed for the human model built from the nAChR template than that built with nAChPB template, and most of the residues are orientated differently. Hence, all comparative models of nAChR species built with the nAChBP template could be far from the real 3D conformation of nAChR.

The binding site of Apis_nAChR$\alpha3\beta2$ is mostly composed of polar and hydrophobic residues, such as serine, threonine, phenylalanine, valine, and tryptophan amino acids. Besides, it is noteworthy that the nature and position of the residues (except for threonine

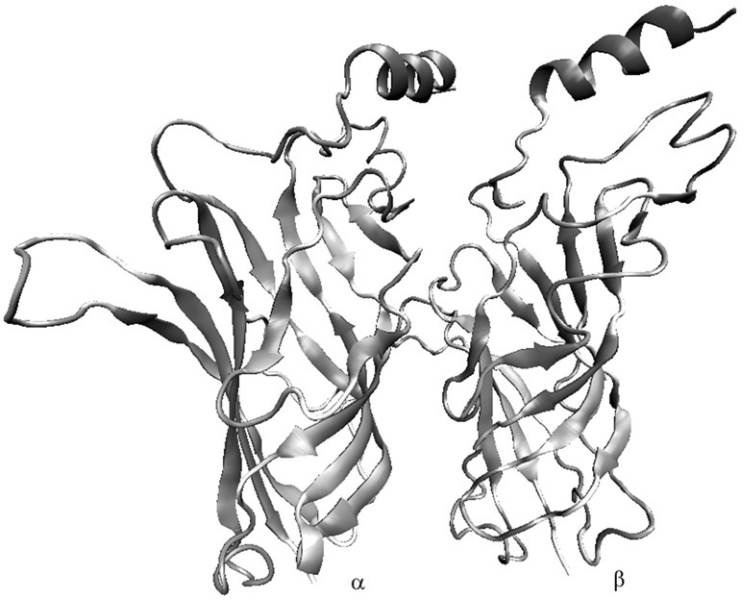

Figure 3. Secondary structure representation of Apis_nAChR$\alpha 3\beta 2$ model with α helices as ribbons and β sheets as arrows.

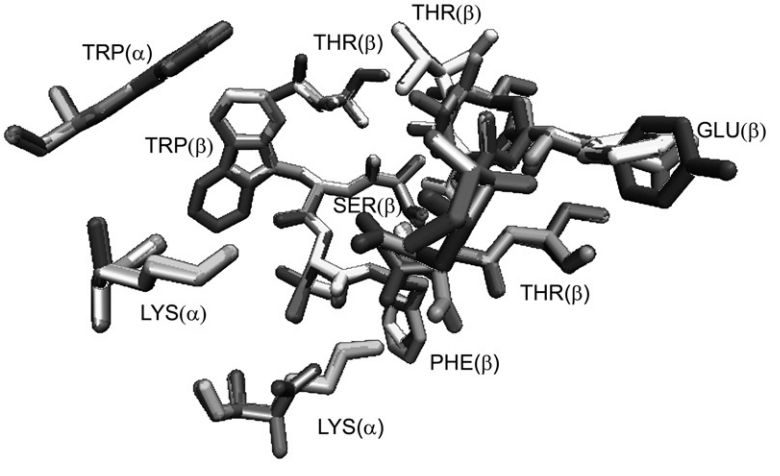

Figure 4. Superposition of binding site residues of Apis_nAChR$\alpha 3\beta 2$ with Apis_nAChR$\alpha 4\beta 2$, Apis_nAChR$\alpha 6\beta 2$, Apis_nAChR$\alpha 9\alpha 9$ and Apis_nAChR$\alpha 1\beta 1$ performed with VMD. The amino acid names belonging to $\alpha 3$ and $\beta 2$ chains are reported respectively with (α) and (β).

and glutamic acid) are conserved in the binding pocket of all homology models with different subunits (Figure 4) [36].

To get insight into the molecular differences between honeybee nAChR (that is supposed to be not targeted by imidacloprid and fipronil) and other insect nAChR targeted by both insecticides, a comparison between their respective receptors has been

```
Alpha3_Bee          YNKLVRPVVNVTDALTVKIKLKLSQLIDVNLKNQIMTTNLWVEQSWYDYKLKWDPKEYGG 60
Alpha3_Flea         YNKLVRPVVNVTDALTVKIKLKLSQLIDVNLKNQIMTTNLWVEQSWYDYKLKWEPKEYGG 60
Alpha3_Aphid        YNKLVRPVLNNTDPLPVRIKLKLSQLIDINLKNQIMTTNLWVEQYWYDYKLTWNPDEYGG 60
Alpha3_Locust       YNRLIRPVGNNSDRLTSKMGLRLSQLIDVNLKNQIMTTNVWVEQEWNDYKLKWNPDDYGG 60
                    **:*:*** * :* *. :: *:******:**********:**** * ****.*:*.:***

Alpha3_Bee          VEMLHVPSDHIWRPDIVLYNNADGNFEVTLATKATLNYTGRVEWKPPAIYKSSCEIDVEY 120
Alpha3_Flea         VEMLHVPSDHIWRPDIVLYNNADGNFEVTLATKATLNYTGRVEWRPPAIYKSSCEIDVEY 120
Alpha3_Aphid        VEGLHVPSEHVWRPDIVLYNNADGNFEVTLATKAMLHYSGRVEWKPPAIYKSSCEIDVEF 120
Alpha3_Locust       VDTLHVPSEHIWLPDIVLYNNADGNYEVTIMTKAILHHTGKVVWKPPAIYKSFCEIDVEY 120
                    *: *****:*:* ************:***: *** *:::*:* *:******* ******:

Alpha3_Bee          FPFDEQTCVMKFGSWTYDGFQVDLRHIDEIRGKNVVDIGVDLSEFYTSVEWDILEVPAVR 180
Alpha3_Flea         FPFDEQTCVMKFGSWTYDGFQVDLRHRDEQTGSNVVDIGIDLSEFYTSVEWDILEVPAVR 180
Alpha3_Aphid        FPFDEQTCVMKFGSWTYDGFQVDLRHANEVSGSRVVDVGVDLSEFYASVEWDILEVPAIR 180
Alpha3_Locust       FPFDEQKCFMKFGSWTYDGYLVDLRHIAQSPDSDTIDVGIDLQDYYLSVEWDIMRVPAVR 180
                    ******.*.**********: *****  :  .. .:*:*:**.::* ******:.***:*

Alpha3_Bee          NEKFYTCCDEPYLDIT 196
Alpha3_Flea         NEKFYTCCDEPYLDIT 196
Alpha3_Aphid        NEKYYTCCEEPYLDIT 196
Alpha3_Locust       NEKFYSCCEEPYPDII 196
                    ***:*:**:*** **
```

Figure 5. CLUSTALW sequence alignment of nAChR $\alpha 3$ subunits of different insect species: *A. mellifera*, *C. felis*, *M. persicae* and *L. migratoria*. Residues pointing toward the active site are highlighted. Stars are under identical amino acids and dots under similar.

carried out. However, there are very few available nAChR sequences for these insects. The sequence search in Swiss-Prot databank led to build only the $\alpha 1/\beta 1$ muscular nAChR, and $\alpha 3$ subunits for *Ctenocephalides felis* (flea), *Myzus persicae* (aphid) and *Locusta migratoria* (locust). A superposition of $\alpha 3$ sequences from these different species with that of *A. mellifera* yielded a high conservation of the active site residues with 96.4% of identity and 98.5% of similarity for the flea, 72.4% of identity and 90.3% of similarity for the locust and 85.7% of identity and 96.9% of similarity for the aphid (Figures 5 and 6). The positively charged lysine residue is the most recurrent residue in these active sites, and is occasionally replaced by the charged arginine residue. All residue natures are represented in the binding site, i.e., positively charged (lysine and arginine), negatively charged (glutamic acid), hydrophobic (triptophan and proline) and polar (serine, glutamine, threonine and asparagine). Hence, this comparison led to the conclusion that a very high sequence homology exists between the four insect nAChR subunits.

4.2 *Docking simulations*

LigandFit parameters were chosen to reproduce the position and orientation of the nicotine within the nAChBP active site found by X-ray structure. A superposition of the X-ray conformation of nicotine and the docked conformation yielded a RMS deviation about 0.38 Å. InsightII was used to investigate the binding modes of ligands into the receptors [33]. The insecticides have different hydrophobic groups that interact with the receptor hydrophobic residues. In addition, insecticides present polar hydrophilic groups that can be accommodated by free spaces of the nAChR active site. To describe how lipophilicity is distributed all over the different parts of the nAChR $\alpha 3/\beta 2$ active site, the molecular lipophilicity potential (MLP) was calculated [37]. The imidacloprid pyridyl

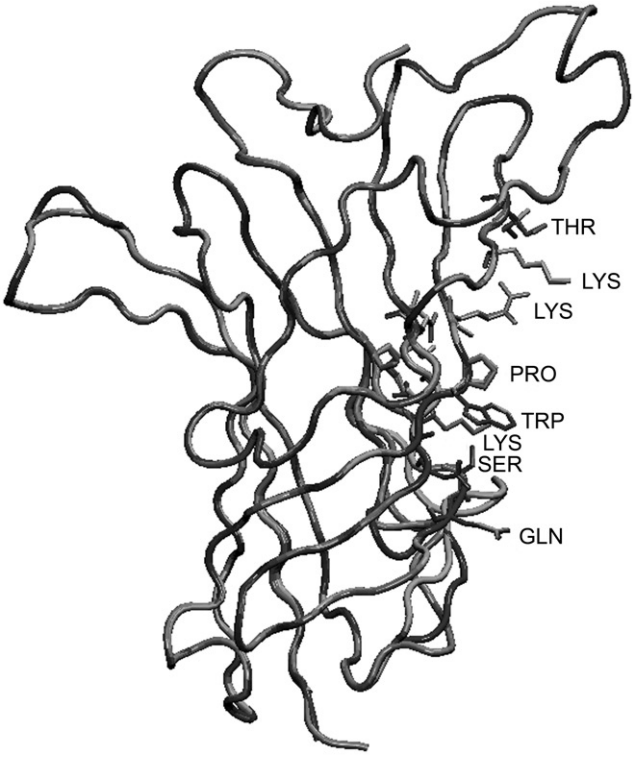

Figure 6. Molecular superposition of $\alpha 3$ comparative models built for the honeybee, the flea, the aphid and the locust.

cycle and the fipronil aromatic cycle are positioned between several hydrophobic surfaces constituted mostly by phenylalanine, tryptophan and leucine amino acids. The polar parts of both insecticides are placed into hydrophilic pockets.

Figure 7 illustrate the docking conformation found for both insecticides and the hydrogen bonds established with the nAChR $\alpha 3/\beta 2$ active site residues. It is worthy to note that imidacloprid is bound with two lysine amino acids and fipronil is involved in five hydrogen bonds with threonine, serine, histidine and one lysine residues. Hence, the docking results revealed that imidacloprid and fipronil (and their metabolites) were able to bind to nAChR. Table 4 summarises the LD_{50} and the number of hydrogen bonds between the insecticides and metabolites and the amino acids of various nAChR subtypes. It can be seen that the hydrogen bond number is slightly correlated with the LD_{50} of *A. mellifera*. In fact, the docking of imidacloprid into nAChR $\alpha 3/\beta 2$ active site revealed three hydrogen bonds while fipronil (lowest LD_{50}) made five hydrogen bonds. The urea and 6-chloronicotinic acid metabolites are involved only into one hydrogen bond, which is in agreement with their high LD_{50}. It appeared that fipronil metabolites established a higher number of hydrogen bonds with $\alpha 3/\beta 2$ and $\alpha 9/\alpha 9$ receptors, and a fewer with the other receptors. Hence, the hypothesis that the heteropentamer subunit types such as $\alpha 4/\beta 2$, $\alpha 6/\beta 2$ and $\alpha 1/\beta 1$ are not targeted by fipronil and its metabolites could be emitted. This study underlines that some residues, present in all receptor subunits, are involved frequently into binding interactions. This is the case for lysine, threonine and serine amino acids, which are found in all honeybee nACh heteropentamer receptor models.

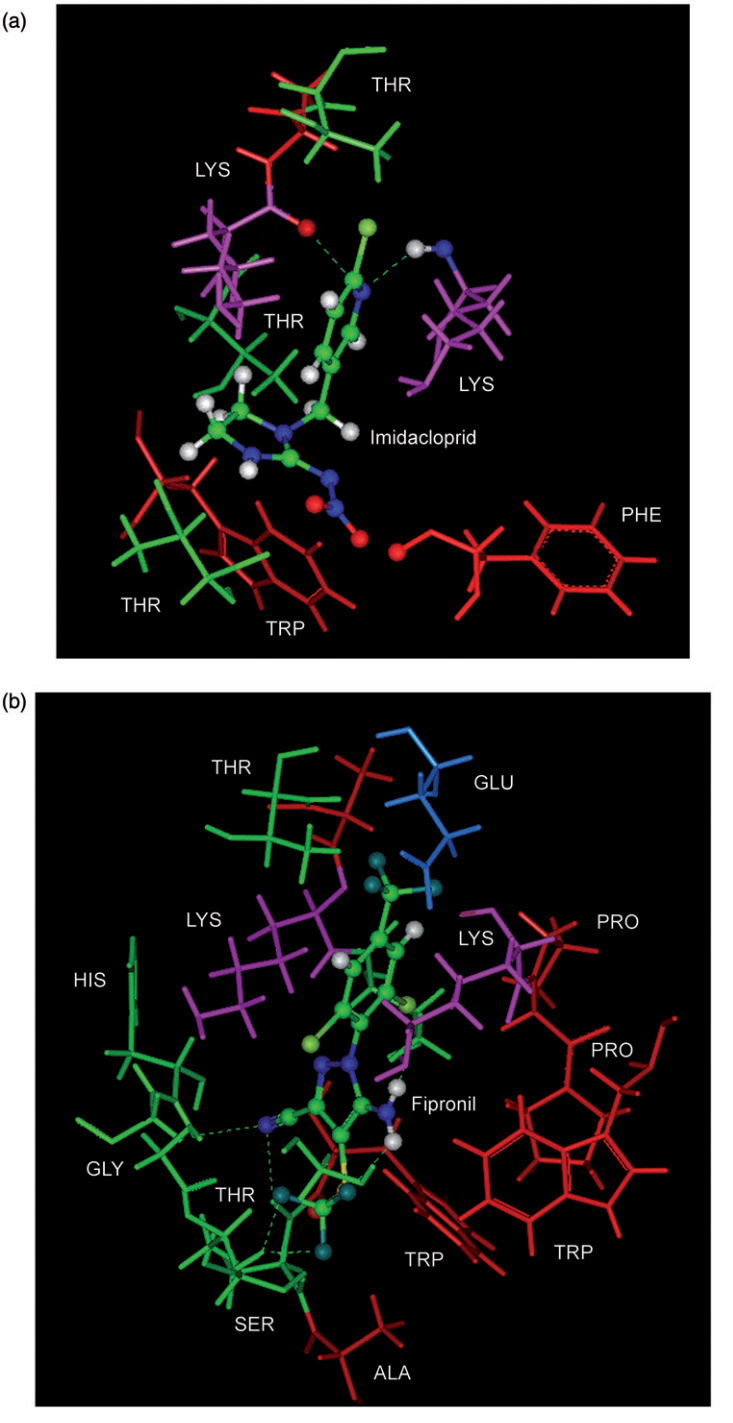

Figure 7. Representation of the docking results into the *A. mellifera* nAChR $\alpha 3/\beta 2$ active site for: (a) Imidacloprid and (b) Fipronil. Hydrogen bonds are coloured in green and residues follow the CLUSTALW colour code: positively charged (magenta), negatively charged (blue), hydrophobic (red) and polar (green).

Table 4. Number of hydrogen bonds between nAChR residues and the docked insecticides.

	Imidacloprid and metabolites							
	Imi	*4OHImi*	*5OHImi*	*DiOHImi*	*Epoxy*	*Olefin*	*Urea*	*6CNA*
LD_{50} ng/bee	41	–	159	>49	–	>36	>99500	>121500
$\alpha3\beta2$	3	6	2	3	5	3	1	1
$\alpha4\beta2$	4	2	4	6	4	2	2	1
$\alpha6\beta2$	1	5	2	3	3	0	2	4
$\alpha1\beta1$	3	1	2	3	3	2	2	2
$\alpha9\alpha9$	5	6	7	5	5	5	2	2

	Fipronil and metabolites										
	Fipronil	*Met 1*	*Met 2*	*Met 3*	*Met 4*	*Met 5*	*Met 6*	*Met 7*	*Met 8*	*Met 9*	*Met 10*
LD_{50} ng/bee	6	–	–	–	–	–	–	–	–	–	–
$\alpha3\beta2$	5	4	5	5	3	3	6	4	3	7	5
$\alpha4\beta2$	3	1	3	2	2	2	5	4	2	1	2
$\alpha6\beta2$	0	1	1	1	0	2	2	1	1	2	1
$\alpha1\beta1$	2	2	2	2	2	3	2	4	2	5	3
$\alpha9\alpha9$	5	6	4	6	5	3	7	4	8	2	3

However, even if some active site residues are conserved from one receptor to another, the number of hydrogen bonds in each one is different. In fact, it appeared that the docked conformations of insecticides are different in each receptor subtype. In addition, these results demonstrate that some metabolites make more hydrogen bonds with the nicotinic receptors than their parent compounds. Moreover, in order to have an idea of the conformational space covered by the docking procedure, the structures of docked insecticides found were superposed into the $\alpha3/\beta2$ nAChR. It was noticed that the pyridyl cycle stays almost in the same place for imidacloprid and its metabolites, and the aromatic cycle moves slightly between fipronil and its metabolites. For the other receptors, imidacloprid metabolites set almost in the same position (except for urea and 6CNA), while the fipronil and its metabolites are barely aligned.

Finally, principal components analysis (PCA) on correlation matrix was performed to find a relationship between the calculated scoring functions and the hydrogen bond number for the receptor subtypes modelled and the LD_{50} of the insecticide compounds selected for this study. Among the heteropentamer subunits, the best results were obtained for the nAChR $\alpha3/\beta2$ subtype, for which the first factorial plan PC1PC2 accounts for 87.61% of the total inertia of the system (Figure 8). The space of the objects (Figure 8a) shows one clusters, which is constituted by the imidacloprid and two of its metabolites of mean LD_{50}. The two most toxic compounds (i.e., fipronil and olefin imidacloprid) are located in the positive part of PC2 axis corresponding to hydrogen bond descriptor (Hbond). This shows that the number of hydrogen bonds is an important factor for the toxicity of compounds. The space of the variables (Figure 8(b)) reveals an opposition between PMF and all other scoring functions. In PC1 axis, urea and 6CNA metabolite compounds of imidacloprid having the greatest LD_{50} are opposed to metabolite compounds of imidacloprid (i.e., 5OH-imidacloprid and diOH-imidacloprid) having the

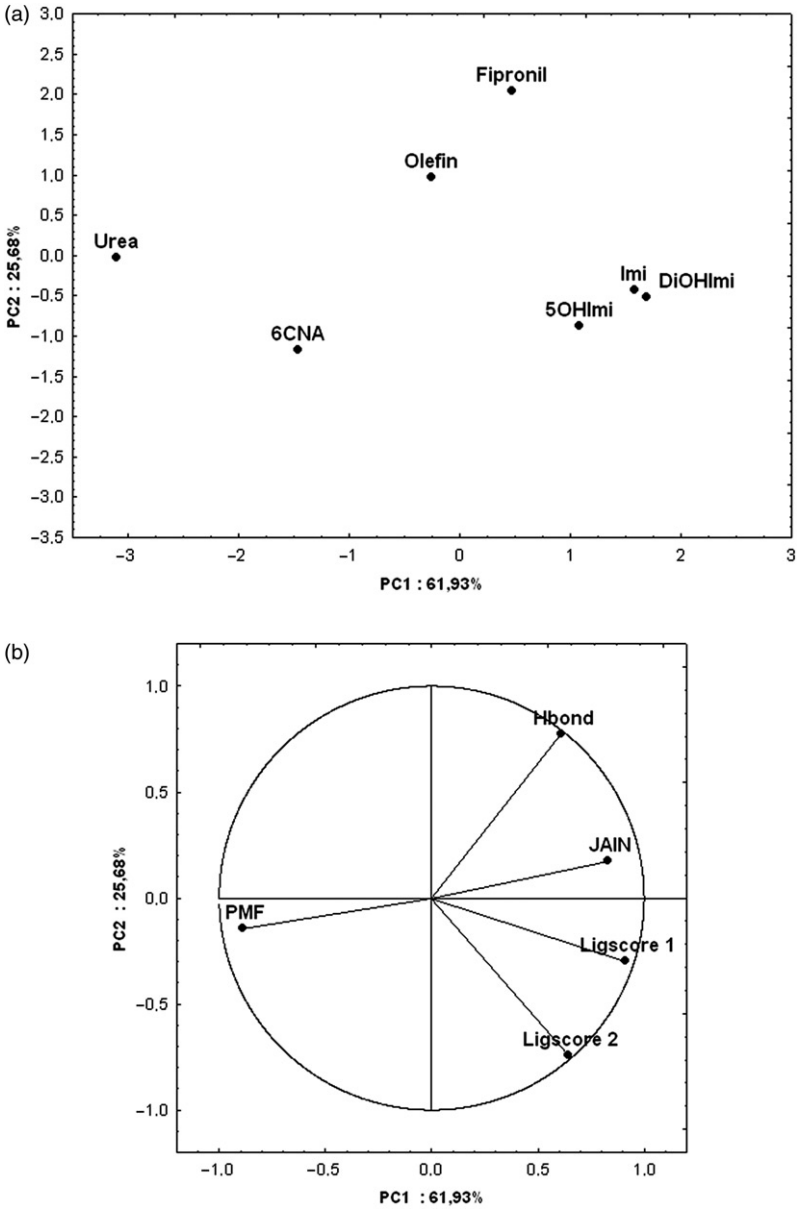

Figure 8. PC1PC2 factorial plan for nAChR $\alpha 3/\beta 2$ subunit. (a) Space of compounds; (b) Space of 3D descriptors.

lowest LD_{50}. Finally, fipronil and most of the imidacloprid metabolites are located in opposite part of PC2 axis. Fipronil and olefin-imidacloprid compounds are more liphophilic than imidacloprid and its two hydroxyl-metabolites. Thus, the position of the three latter ''polar'' compounds in the PC1PC2 factorial plan, is due to the Ligscore functions, which consist of distinct terms describing the van der Waals interaction, the polar attraction between the ligand and protein, and the desolvation penalty attributed to

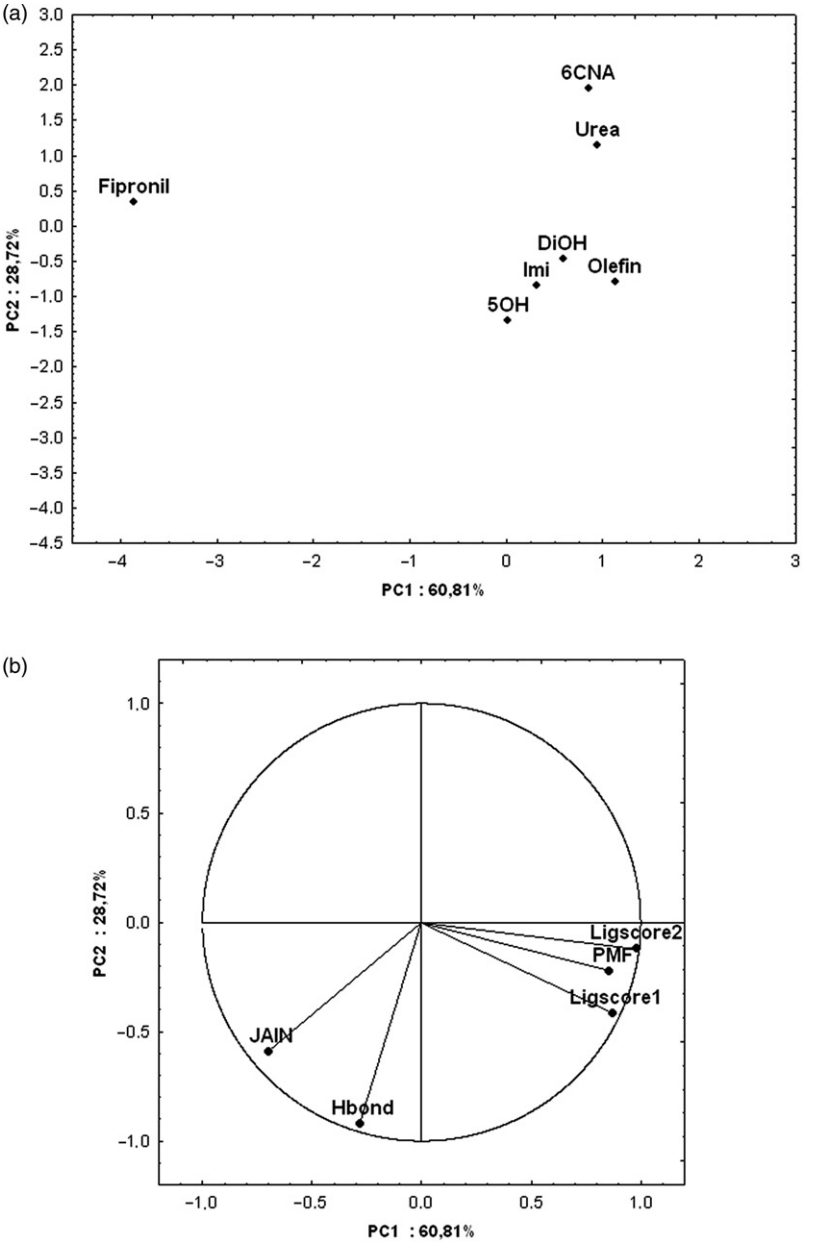

Figure 9. PC1PC2 factorial plan for nAChR $\alpha 9/\alpha 9$ subunit. (a) Space of compounds; (b) Space of 3D descriptors.

the binding of the polar ligand atoms to the protein. Conversely, the position of olefin (most hydrophobic metabolite of imidacloprid of known LD_{50}) is caused by the Jain scoring function, which is an empirical scoring function consisting of hydrophobic and polar terms, as well as terms for entropic and solvation effects. This 3D descriptor is responsible to drive the olefin compound higher in the PC2 axis compared to the other

imidacloprid metabolites. The position of urea and 6CNA is driven by the PMF scoring function, which is a distance-dependent Helmholtz free interaction energy of protein-ligand atom pairs corrected by a ligand volume factor to filter out intramolecular ligand interactions [38]. For the $\alpha 9/\alpha 9$ nAChR homopentamer, the first factorial plan PC1PC2 accounts for 89.53% of the total inertia of the system (Figure 9). As previously noted, the 3D descriptors chosen such as Hbond, Ligscore 1 and 2 are able to differentiate imidacloprid metabolites having low LD_{50} from the compounds with high LD_{50} (i.e., urea and 6CNA metabolites).

It is noteworthy that from a structure-activity point of view, the calculated scoring functions and hydrogen bonds are interesting descriptors to get insight into the toxicity mechanism of insecticides for a selected receptor. This qualitative analysis shows that insecticide toxicities seem to be governed by the binding features to *A. mellifera* nAChR $\alpha 3/\beta 2$ and $\alpha 9/\alpha 9$ subtypes, such as hydrogen bond number and polar/hydrophobic interactions.

5. Conclusions

This study presents five different honeybee *Apis mellifera* nACh receptor subtypes obtained by homology modelling with the recent crystal structure of *Torpedo marmorata* nAChR. The docking of imidacloprid and metabolites into the honeybee nAChR active site reveals numerous hydrogen bonds and hydrophobic interactions. It appears that a compound with a low LD_{50} is making a large number of hydrogen bond into the active site of nAChR $\alpha 3/\beta 2$. However, the neurotoxic insecticides and their metabolites seem to make few hydrogen bonds with the $\alpha 4/\beta 2$, $\alpha 6/\beta 2$ and $\alpha 1/\beta 1$ nAChR subtypes compared to $\alpha 3/\beta 2$ and $\alpha 9/\alpha 9$ subunits. This study evidences the fact that both insecticides and metabolites could bind with the honeybee nAChR. Moreover, it appears that interactions between fipronil metabolites and nicotinic acetylcholine receptor subtypes such as $\alpha 3/\beta 2$ and $\alpha 9/\alpha 9$ are not negligible. These results reveal that accidental and/or long exposition to imidacloprid and fipronil would result in a risk for honeybee health. Furthermore, from the principal components analysis, it appears that the calculated scoring functions and the number of hydrogen bonds are able to distinguish molecules with low LD_{50} from those with high LD_{50}.

References

[1] L.A. Brown, M. Ihara, S.D. Buckingham, K. Matsuda, and D.B. Sattelle, *Neonicotinoid insecticides display partial and super agonist actions on native insect nicotinic acetylcholine receptors*, J. Neurochem. 99 (2006), pp. 608–615.

[2] M. Tomizawa and J.E. Casida, *Minor structural changes in nicotinoid insecticides confer differential subtype selectivity for mammalian nicotinic acetylcholine receptors*, Br. J. Pharmacol. 127 (1999), pp. 115–122.

[3] S. Suchail, G. De Sousa, R. Rahmani, and L.P. Belzunces, *In vivo distribution and metabolisation of 14C-imidacloprid in different compartments of Apis mellifera L.*, Pest Manag. Sci. 60 (2004), pp. 1056–1062.

[4] D. Guez, *Effets sublétaux de l'imidaclopride sur le comportement de l'abeille domestique (Apis mellifera)*, Ph.D. diss., Pierre and Marie Curie University, 2001.

[5] N. Unwin, *Refined structure of the nicotinic acetylcholine receptor at 4 Å resolution*, J. Mol. Biol. 346 (2005), pp. 967–989.

[6] T. Schwede, J. Kopp, N. Guex, and M.C. Peitsch, *SWISS-MODEL: an automated protein homology-modeling server*, Nucleic Acids Res. 31 (2003), pp. 3381–3385. Available at http://swissmodel.expasy.org/SWISS-MODEL.html (Accessed 4 July 2007).
[7] *Cerius*^{2} 4.7, Accelrys Inc., USA.
[8] K. Jozwiak, S. Ravichandran, J.R. Collins, and I.W. Wainer, *Interaction of noncompetitive inhibitors with an immobilized α3β4 nicotinic acetylcholine receptor investigated by affinity chromatography, quantitative-structure activity relationship analysis, and molecular docking*, J. Med. Chem. 47 (2004), pp. 4008–4021.
[9] A. Mourot, *Structure et Dynamique du Récepteur Nicotinique*, PhD diss., Louis Pasteur University, 2004.
[10] S.H. Thany, M. Crozatier, V. Raymond-Delpech, M. Gauthier, and G. Lenaers, *Apisalpha2, apisalpha7-1 and apisalpha7-2: three new neuronal nicotinic acetylcholine receptor alpha-subunits in the honeybee brain*, Gene 344 (2005), pp. 125–132.
[11] A.K. Jones, V. Raymond-Delpech, S.H. Thany, M. Gauthier, and D.B. Sattelle, *The nicotinic acetylcholine receptor gene family of the honey bee, Apis mellifera*, Genome Res. 16 (2006), pp. 1422–1430.
[12] A.K. Jones and D.B. Sattelle, *The cys-loop ligand-gated ion channel superfamily of the honeybee, Apis mellifera*, Invertebr. Neurosci. 6 (2006), pp. 123–132.
[13] P.H. Celie, S.E. van Rossum-Fikkert, W.J. van Dijk, K. Brejc, A.B. Smit, and T.K. Sixma, *Nicotine and carbamylcholine binding to nicotinic acetylcholine receptors as studied in AChBP crystal structures*, Neuron. 41 (2004), pp. 907–914.
[14] K. Brejc, W.J. van Dijk, R.V. Klaasen, M. Schuurmans, J. van der Oost, A.B. Smit, and T.K. Sixma, *Crystal structure of an ACh-binding protein reveals the ligand-binding domain of nicotinic receptors*, Nature 441 (2001), pp. 269–276.
[15] S. Dutertre, A. Nicke, J.D.A. Tyndall, and R.J. Lewis, *Determination of α-conotoxin binding modes on neuronal nocotinic acetylcholine receptors*, J. Mol. Recognit. 17 (2004), pp. 339–347. Available at: www.imb.uq.edu.au/index.html?page = 15581&pid = 12142 (Accessed 11 February 2007).
[16] Z. Pei, L. Yitong, L. Baofeng, and J.J. Gan, *Dynamics of fipronil residue in vegetable-field ecosystem*, Chemosphere 57 (2004), pp. 1691–1696.
[17] R. Nauen, U. Ebbinghaus-Kintscher, and R. Schmuck, *Toxicity and nicotinic acetylcholine receptor interaction of imidacloprid and its metabolites in Apis mellifera (Hymenoptera: Apidae)*, Pest. Manag. Sci. 57 (2001), pp. 577–586.
[18] A. Decourtye, *Etude de l'impact de produits phytopharmaceutiques sur la survie et l'apprentissage associatif chez l'abeille domestique (Apis mellifera L.)*, PhD diss., Paris XI University, 2002.
[19] AMPAC 8.16, Semichem Inc., USA.
[20] Gaussian 98, Gaussian Inc., USA.
[21] F.H. Allen, *The Cambridge Structural Database: a quarter of a million crystal structures and rising*, Acta Cryst. B 58 (2002), pp. 380–388.
[22] N. Guex and M.C. Peitsch, *SWISS-MODEL and the Swiss-PdbViewer: an environment for comparative protein modelling*, Electrophoresis 18 (1997), pp. 2714–2723. Available at http://www.expasy.org/spdbv/ (Accessed 4 July 2007).
[23] E. Gasteiger, A. Gattiker, C. Hoogland, I. Ivanyi, R.D. Appel, and A. Bairoch, *ExPASy: the proteomics server for in-depth protein knowledge and analysis*, Nucleic Acids Res. 31 (2003), pp. 3784–3788. Available at http://www.expasy.org/spdbv/ (Accessed 4 July 2007).
[24] B. Boeckmann, M.C. Blatter, L. Famiglietti, U. Hinz, L. Lane, B. Roechertand, and A. Bairoch, *Protein variety and functional diversity: Swiss-Prot annotation in its biological context*, C. R. Biol. 328 (2005), pp. 882–899. Available at http://www.ebi.ac.uk/swissprot/ (Accessed 4 July 2007).
[25] R. Chenna, H. Sugawara, T. Koike, R. Lopez, T. Gibson, D. Higgins, and J. Thompson, *Multiple sequence alignment with the Clustal series of programs*, Nucleic Acids Res. 31 (2003), pp. 3497–3500. Available at http://www.ebi.ac.uk/clustalw/ (Accessed 4 July 2007).

[26] W.R.P. Scott, P.H. Hünenberger, I.G. Tironi, A.E. Mark, S.R. Billeter, J. Fennen, A.E. Torda, T. Huber, P. Krüger, and W.F. van Gunsteren, *The GROMOS Biomolecular Simulation Program Package*, J. Phys. Chem. A 102 (1999), pp. 3596–3607.
[27] P. Dauber-Osguthorpe, V.A. Roberts, D.J. Osguthorpe, J. Wolff, M. Genest, and A.T. Hagler, *Structure and energetics of ligand binding to proteins: Escherichia coli dihydrofolate reductase-trimethoprim, a drug-receptor system*, Proteins Struct. Funct. Genet. 4 (1988), pp. 31–47.
[28] C.M. Venkatachalam, X. Jiang, T. Oldfield, and M. Waldman, *LigandFit: a novel method for the shape-directed rapid docking of ligands to protein active sites*, J. Mol. Graph. Model. 21 (2003), pp. 289–307.
[29] A. Krammer, P.D. Kirchhoff, X. Jiang, C.M. Venkatachalam, and M. Waldman, *Ligscore: a novel scoring function for predicting binding affinities*, J. Mol. Graph. Model. 23 (2005), pp. 395–407.
[30] D.K. Gehlhaar, D. Bouzida, and P.A. Rejto, *Rational Drug Design: Novel Methodology and Practical Applications*, American Chemical Society, Washington, 1999.
[31] A.N. Jain, *Scoring noncovalent protein-ligand interactions: a continuous differentiable function tuned to compute binding affinities*, J. Comput. -Aided Mol. Des. 10 (1996), pp. 427–440.
[32] I. Muegge and Y.C. Martin, *A General and fast scoring function for protein-ligand interactions: a simplified potential approach*, J. Med. Chem. 42 (1999), pp. 791–804.
[33] InsightII 2000, Accelrys Inc., USA.
[34] N. Marchand-Geneste and A. Rocher, *Potential toxic risk of neurotoxic insecticide metabolites on honeybee and human nervous system. A SAR investigation*, SETAC Europe 17th Annual Meeting, Porto, 2007.
[35] N. Marchand-Geneste and A.J.M. Carpy, *Interactions between two neurotoxic insecticides, imidacloprid and fipronil, and human nACh and GABAA Receptors: potential risk on human health*, 12th International Workshop on Quantitative Structure-Activity Relationships in Environmental Toxicology, Lyon, 2006.
[36] W. Humphrey, A. Dalke, and K. Schulten, *VMD: visual molecular dynamics*, J. Mol. Graph. 14 (1996), pp. 33–38.
[37] E. Audry, J.P. Dubost, J.C. Colleter, and P. Dallet, *A new approach to structure-activity relations: the molecular lipophilicity potential*, Eur. J. Med. Chem. 21 (1986), pp. 71–72.
[38] I. Muegge, *Effect of ligand volume correction on PMF scoring*, J. Comput. Chem. 22 (2001), pp. 418–425.